Supplemental Materials

Figure S1

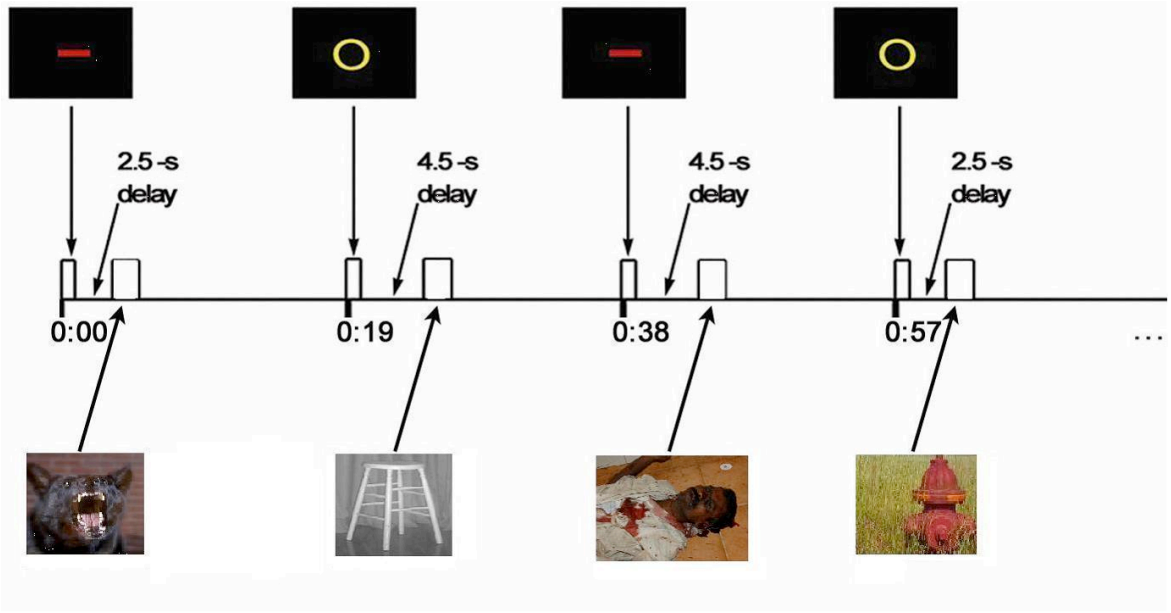

Figure S2

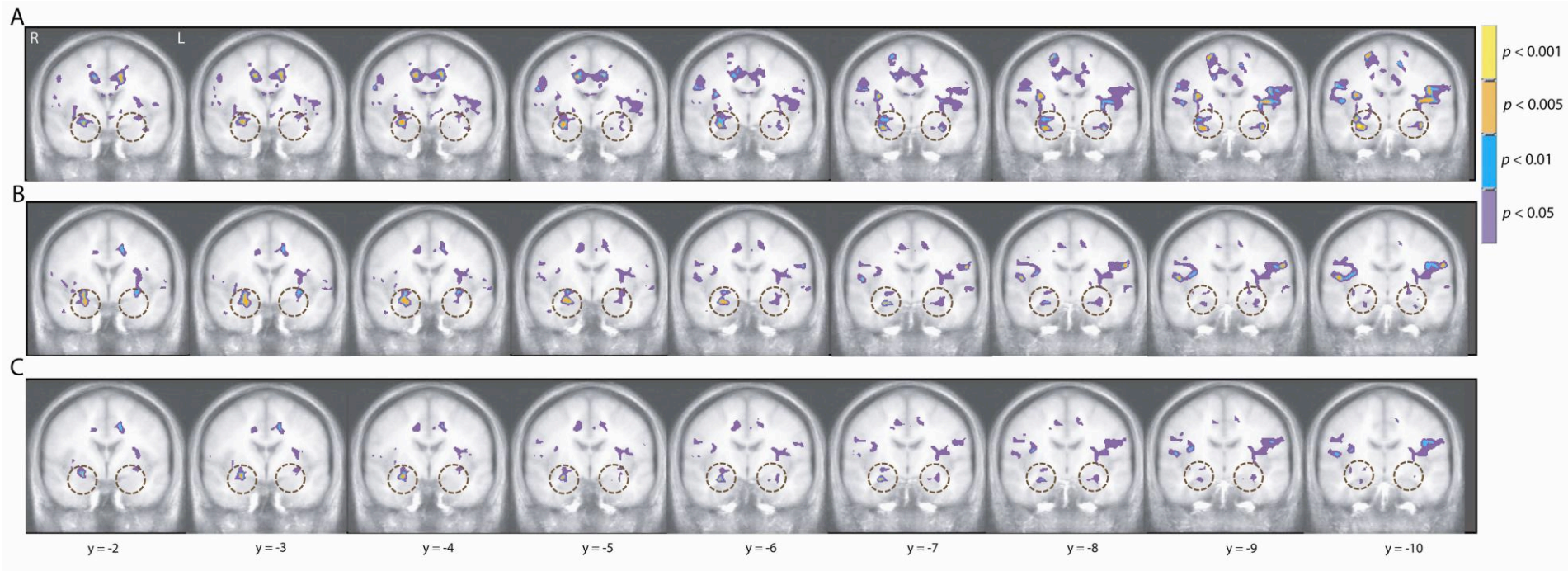

Figure S3

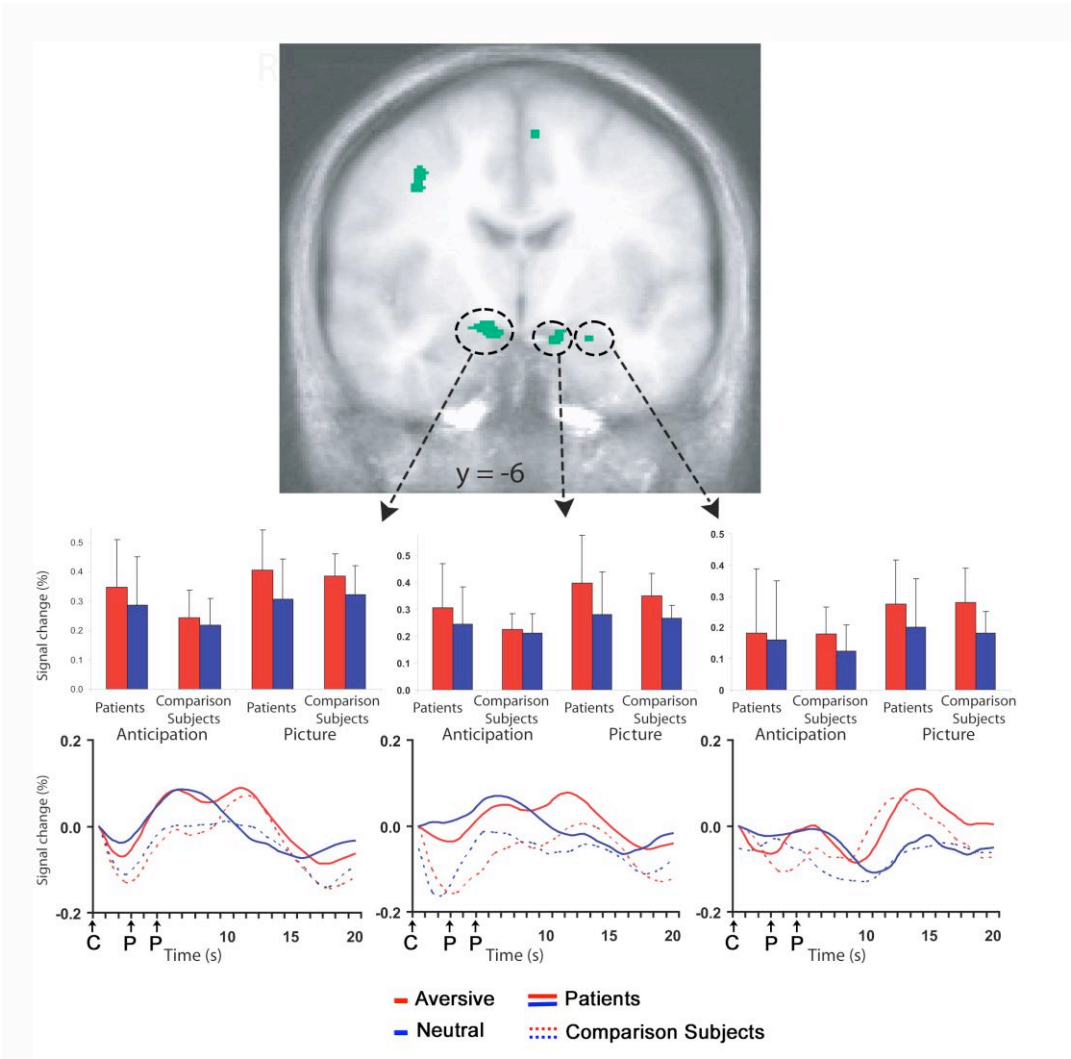
y = -6
Signal change (%)
Patients
Comparison Subjects
Anticipation
Picture
Time (s)
C
P
Aversive
Neutral
Patients
Comparison Subjects

Supplemental Figure Titles and Footnotes

Figure S1. Event-related fMRI paradigm[a].

[a]Presentation of a 0.5-s visual cue at the beginning of a trial preceded the presentation of a 1-s picture after an interval of 2.5 or 4.5 s. A minus sign invariably preceded aversive pictures, and a circle invariably preceded neutral pictures. Subjects were allowed to close their eyes during the 13-s or 15-s black screen that ended each 19-s trial, and a tone was presented over headphones 1 s prior to the onset of each warning cue to signal the subjects to open their eyes and prepare for the next trial. All pictures used were from the International Affective Picture Set (IAPS; 1) and were shown only once. Based on published norms (1), pictures rated as most unpleasant and arousing comprised the aversive set, which primarily included photographs of mutilated bodies and attack scenes. Pictures with neutral valence and low arousal ratings were selected for the neutral pictures (e.g., household items). Of the 104 total pictures, 48 aversive pictures were presented on aversive trials, and 48 neutral pictures were presented on neutral trials. The remaining 8 pictures (4 aversive and 4 neutral) were presented on mismatch trials that were excluded from analyses. For copyright reasons, pictures shown here are not from the IAPS but are in the public domain and were selected to be highly similar to IAPS pictures used in this study. The epoch between the cue and picture was kept short to minimize any working memory component that might interfere with the reaction to the cue. Consistent with a prior study in our lab (2), the use of either 2.5 or 4.5 s as the delay between the cue and picture allowed differentiation of the hemodynamic response due to the cue from that due to the picture. The longer delay following the picture allowed the hemodynamic response to the picture to return to baseline before the onset of the subsequent cue.

1. Lang PJ, Bradley MM, Cuthbert BN: International affective picture system (IAPS): instruction manual and affective ratings. Gainesville, FL: University of Florida; 1999.
2. Nitschke JB, Sarinopoulos I, Mackiewicz KL, Schaefer HS, Davidson RJ: Functional neuroanatomy of aversion and its anticipation. Neuroimage 2006; 29(1):106-116.

Figure S2. Intensity maps for brain activations during the anticipation of aversive and neutral pictures[a].

[a]Brain images intersecting the amygdala are shown for areas with greater activation for GAD patients (N=14) than healthy comparison subjects (N=12) in anticipation of aversive pictures (A), in anticipation of neutral pictures (B), and their overlap (C). Controls did not show greater activation than GAD patients in any amygdala (or insula) areas. Circles indicate the approximate locations of the amygdalae on each slice. The view of the brain shown is indicated by the relevant Talairach coordinate at the bottom of each column.

Figure S3. Greater amygdala activity in anticipation of and response to aversive than neutral pictures[a].

[a]All subjects showed greater bilateral amygdala activation on aversive than neutral trials across both anticipation and picture periods, as indicated by a Valence main effect (green) for a voxelwise Group x Valence x Period ANOVA (N=26; $p<0.05$, corrected; Table 2; Figure 1). Bar graphs of the circled clusters for the Valence effect illustrate average percentage signal change for the anticipation and picture periods. The data depicted in the brain images and bar graphs are beta-weights indicating fit to an ideal hemodynamic response. The time series were derived from deconvolved estimates for display purposes only. Time series plots of the circled clusters illustrate average percentage signal change across all time points of the aversive (red) and neutral

(blue) trials for GAD patients (solid lines) and healthy comparison subjects (dotted lines) separately. The onset of the 1-s picture (P) occurred 3 s after cue (C) onset on half of the trials and 5 s after cue onset on the other half. Error bars for bar graphs are for SD. R = right. L = left.

Table S1. Correlations among symptom measures.

Instrument	Ham-A	Ham-D
fMRI Session (Pretreatment)		
Ham-D	0.63	
PSWQ	0.27	0.20
Week 8 Session (Posttreatment)		
Ham-D	0.69	
PSWQ	0.89	0.49

Note. All correlations are for generalized anxiety disorder patients only, excluding one patient who did not complete the study (N=13). Ham-A = Hamilton Rating Scale for Anxiety. Ham-D = Hamilton Rating Scale for Depression. PSWQ = Penn State Worry Questionnaire.

Table S2. Brain regions showing activation differences for anticipating and viewing emotional pictures in healthy comparison subjects.

	Talairach Coordinates				
Brain Region	*x*	*y*	*z*	Size (mm^3)	*F* value
R Amygdala	25	-7	-18	503	18.422
L Amygdala	-24	-9	-14	65	15.944
L Amygdala	-25	0	-20	91	18.091
R Anterior Hippocampus	24	-25	-12	195	18.539
R Anterior Hippocampus	22	-28	-3	73	14.601
R Anterior Insula/Inferior Frontal Gyrus	30	22	-1	3707	20.334
L Anterior Insula	-31	21	-2	1429	17.268
Supragenual Anterior Cingulate Cortex	4	46	17	2733	18.748
R Orbitofrontal Cortex	32	27	-12	163	19.031

Note. Table displays regions that showed greater activation to the aversive than neutral trials for the healthy comparison subjects (N=12), as indicated by the Valence main effect of a voxelwise Valence (Aversive, Neutral) x Period (Anticipation, Picture) ANOVA, replicating our earlier reports (8,17). All listed clusters were significant at $p<0.05$ (corrected). *F* values for ANOVA effects are for entire cluster. R = right. L = left.

Table S3. Brain regions showing activation differences when anticipating and viewing emotional pictures using previously reported functionally defined regions of interest.

	GAD vs. Healthy Comparison Subjects								Comparison Subjects	
	Anticipation Period				Picture Period				Both Periods	
	Group Effect		Group x Valence		Group Effect		Group x Valence		Valence Effect	
Brain Region	*F*	*p*	*F*	*p*	*F*	*p*	*F*	*p*	*F*	*p*
R Dorsal Amygdala	2.26	0.15	0.31	0.58	0.66	0.42	3.67	0.07	6.25	0.03
L Dorsal Amygdala	2.46	0.13	0.06	0.81	0.61	0.44	1.25	0.27	5.74	0.04
R Anterior Hippocampus	3.79	0.06	1.30	0.27	0.59	0.45	1.03	0.32	1.84	0.20
L Anterior Hippocampus	3.73	0.06	0.81	0.38	0.23	0.64	3.59	0.07	3.70	0.08
R Anterior Insula	1.16	0.29	0.38	0.54	0.20	0.66	0.01	0.91	18.74	0.001
L Anterior Insula	2.45	0.13	0.78	0.39	0.00	0.98	0.31	0.58	15.34	0.002
Supragenual ACC	0.27	0.61	1.67	0.21	0.33	0.86	0.22	0.65	17.21	0.002
R Posterior OFC	1.42	0.25	3.95	0.06	0.09	0.77	2.42	0.13	0.05	0.83
R Anterior DLPFC	3.19	0.09	0.72	0.40	1.03	0.32	0.08	0.78	1.19	0.30
R Posterior DLPFC	0.66	0.43	0.02	0.89	0.03	0.87	0.01	0.91	7.74	0.02

Note. Results for Group Effect and Group x Valence refer to the corresponding main and interaction effects for Group (Patients, Comparison Subjects) x Valence (Aversive, Neutral) MANOVAs using all subjects (N=26) conducted separately for each period (anticipation, picture) and for each functionally defined region of interest reported previously (8). Results for Valence Effect refer to the corresponding main effect for Valence (Aversive, Neutral) x Period (Anticipation, Picture) MANOVAs on healthy comparison subjects (N=12) conducted separately for each functionally defined region of interest reported previously (8). *P* values were not corrected for multiple comparisons. R = right. L = left. ACC = anterior cingulate cortex. OFC = orbitofrontal cortex. DLPFC = dorsolateral prefrontal cortex.

Supplemental Methods

To assess the extent of signal loss resulting from differential magnetic susceptibility coefficients at bone/air/tissue boundaries, we calculated signal-to-noise ratios (SNR) in all amygdala clusters identified in this report. For comparison purposes, we calculated SNR from anatomically defined clusters in regions with minimal signal loss, including the superior frontal gyrus, precentral gyrus, and precuneus. SNR was determined independently for each voxel by dividing the mean time series signal by the standard deviation of that time series signal. Regional SNR estimates were obtained by averaging across voxels in each amygdala cluster found here. Adequate signal was observed for all identified amygdala clusters in all subjects. SNR values ranged from 35 to 76 for the amygdala clusters implicated in the present study and from 58 to 81 for clusters in the superior frontal, precentral, and precuneus control regions.

Approximately one week before the fMRI session, all subjects were positioned in a mock MRI scanner, including head coil, goggles, bite bar, response box, and digitized scanner sounds presented over headphones. While in the mock scanner, subjects were instructed about the experimental task, including the cue-picture pairing, and then viewed an abbreviated version of the paradigm with different pictures than those shown during the fMRI session. This simulation session served to acclimate subjects to the fMRI environment, to further assess for claustrophobia, to ascertain that aversive pictures were tolerable, and to reinforce the cue-picture pairing.

Supplemental Results

Ancillary analyses were conducted to further explore ACC associations with treatment response. For the Ham-A, nearly identical ACC areas to that shown in Figure 2A were observed for regressions using other commonly employed treatment response metrics: pretreatment – posttreatment difference scores (r=0.85; 409 mm^3; x=-1, y=35, z=19) and (pretreatment – posttreatment)/pretreatment scores (r=0.83; 453 mm^3; x=-1, y=34, z=19). For the ACC area shown in Figure 2A, associations with treatment response were observed for ACC activity in anticipation of aversive pictures alone (r=-0.75) and in anticipation of neutral pictures alone (r=-0.69). This pattern was confirmed by voxelwise regressions conducted separately for the aversive and neutral conditions, with activations in the same ACC area for the anticipation of aversive pictures (347 mm^3; x=1, y=32, z=19) and for the anticipation of neutral pictures, albeit smaller (62 mm^3; x=-6, y=32, z=20). Similar associations with the Ham-A for the conditions separately were observed for the two alternate treatment response metrics.

For the PSWQ, nearly identical ACC areas to that shown in Figure 2B were observed for regressions using other commonly employed treatment response metrics: pretreatment – posttreatment difference scores (r=0.84; 93 mm^3; x=-3, y=38, z=15) and (pretreatment – posttreatment)/pretreatment scores (r=0.84; 172 mm^3; x=-4, y=41, z=17). For the ACC area shown in Figure 2B, associations with treatment response were observed for ACC activity in anticipation of aversive pictures alone (r=-0.80) and in anticipation of neutral pictures alone (r=-0.68. This pattern was confirmed by voxelwise regressions conducted separately for the aversive and neutral conditions, with activations in the same ACC area for the anticipation of aversive pictures (539 mm^3; x=2, y=32, z=22) and for the anticipation of neutral pictures, albeit smaller (50 mm^3; x=3, y=31, z=20). Similar associations with the PSWQ for the conditions separately were observed for the two alternate treatment response metrics.